South Asian J. Zool., vol. 44(2), pp 115-122, 2026 DOI: https://dx.doi.org/10.17582/sajz/2026/44.2.115.122



In Silico Identification and Characterization of Phytochemicals from *Digera arvensis* as Potential Carbonic Anhydrase IX (CAIX) Inhibitors

Shahid Ullah[1], Erum Zafar[1], Qurban Ali[1], Muhammad Tayyab Waqar[2] and Muhammad Khan[1]*

[1]*Cancer Research Lab, Institute of Zoology, University of the Punjab, Quaid-e-Azam Campus, Lahore 54590, Pakistan*
[2]*Department of Computer Science, University of Management and Technology, Sialkot, Pakistan*

Shahid Ullah and Erum Zafar contributed equally in this manuscript.

Article Information
Received 27 September 2026
Revised 25 October 2026
Accepted 11 November 2026
Available online 23 November 2026

Authors' Contribution
SU: Investigation, methodology, visualization, writing original draft. EZ: Investigation, methodology, formal analysis, data curation, writing-original draft. QA: Data curation, formal analysis, software, writing, review and editing. MTW: Methodology, validation, visualization. MK: Conceptualization, supervision, project administration, resources, writing, review and editing.

Key words
Breast cancer, Carbonic anhydrase, CAIX, *Digeria arvensis*, Molecular docking

ABSTRACT

Carbonic Anhydrase IX (CAIX), a zinc-containing transmembrane hypoxia-induced enzyme is critical for controlling tumor pH and enhancing viability of cancer cells. CAIX could be a good target for cancer drug development, because it is over-expressed in hypoxic tumors. In the present study, we aimed to explore the inhibitory potential of phytochemicals isolated from *Digera arvensis* against human CAIX (PDB ID: 8Q18) via molecular docking, drug likeness and ADMET analyses. 1,3-Benzenedicarboxylic acid, bis(2-ethylhexyl) ester and Bis(2-ethylhexyl) phthalate, was the top leading compounds with a docking score of −7.9kcal/mol and Ki value of 1.62µM among the selected phytochemicals. The compound showed favourable hydrogen bonding and hydrophobic interactions within the active site of CAIX. All the ligands showed favorable pharmacokinetic properties, drug-likeness and ADMET analysis, which showed good intestinal absorption, no hepatotoxicity and AMES toxicity, and no CYP450 inhibition. These findings identify the compounds as computational hits only; experimental validation of CAIX inhibition and a thorough toxicological evaluation are required before any therapeutic consideration.The results indicate that the phytochemicals present in *Digera arvensis* could be valuable lead molecules for future *in-vitro* and *in-vivo* studies to be explored as anticancer agents against CAIX.

INTRODUCTION

Carbonic Anhydrase IX (CAIX) is a hypoxia-inducible, transmembrane zinc metalloenzyme whose catalytic domain faces the extracellular space. It catalyzes the reversible hydration of carbon dioxide to bicarbonate and a proton ($CO_2 + H_2O \rightleftharpoons HCO_3^- + H^+$). At the cell surface, the protons generated remain in the extracellular compartment and acidify it, while the bicarbonate is taken up into the cell through bicarbonate transporters. This helps maintain a neutral to slightly alkaline intracellular pH in tumor cells despite their high glycolytic acid load (Supuran, 2023; Mboge *et al*., 2022). Tumor hypoxia is identified as a hallmark of aggressive cancers and is an important factor in cancer progression, metastasis, resistance and poor prognosis (Rankin and Giaccia, 2022; Vaupel and Multhoff, 2022). When oxygen levels are low, the cancer cells adapt by expressing hypoxia-inducible factor-1 alpha (HIF-1α), leading to increased angiogenesis, metabolic reprogramming, and tumor survival (Semenza, 2022; Jing *et al*., 2023).

CAIX is minimally expressed in normal tissues but is highly overexpressed in several solid tumors such as breast, lung, colorectal, renal and cervical cancers (Pastorekova *et al*., 2023; McDonald *et al*., 2023). By acidifying the extracellular microenvironment while supporting intracellular pH homeostasis, CAIX promotes tumor cell survival, invasion and metastasis, and contributes to resistance to chemotherapy and radiotherapy (Alterio *et al*., 2022; Supuran, 2023). CAIX is a potential tumor-specific marker for tumor hypoxia and a potential

* Corresponding author: mkhan.zool@pu.edu.pk
1013-3461/2026/0001 $ 0.00/0

Copyright 2026 by the authors.
This article is an open access article distributed under the terms and conditions of the Creative Commons Attribution (CC BY) license (https://creativecommons.org/licenses/by/4.0/).

therapeutic target for the development of anticancer drugs, and it is highly expressed in hypoxic tumors (Cheung and Chenoweth, 2023). CAIX is a transmembrane member of the α-carbonic anhydrase family. It consists of a catalytic domain containing a zinc ion, a proteoglycan-like domain, a transmembrane domain and an intracellular tail (Supuran, 2008; Alterio *et al*., 2009).

This structural diversity and biological activities of natural products from medicinal plants have generated considerable interest in the search of safe and potent anticancer drugs from these plants (Kumar *et al*., 2023; Zhang *et al*., 2024). *Digera arvensis*, also known as False Amaranth or Tandla, is a member of Amaranthaceae family and widely distributed in tropical and subtropical countries like Pakistan, India, Bangladesh, Africa and Middle East. It has bioactive phytochemicals such as flavonoids, alkaloids, phenolic compounds, and saponins with antimicrobial, antioxidant, anti-inflammatory, and anticancer activities (Rahman *et al*., 2023; Ali *et al*., 2024).

With the benefit of accelerated research and development, computational or *in silico* methods like molecular docking and ADMET prediction have gained significant importance in recent years for bioactivity screening of compounds and for their role in the identification of candidate drugs in the drug discovery process (Patel *et al*., 2023; Ferreira *et al*., 2022). The molecular docking study is useful in predicting the interaction and binding capacity of the ligand to protein, while the ADMET study is helpful for studying the pharmacokinetic and toxic properties required for drug development (Khan *et al*., 2024; Lionta *et al*., 2023).

The present study is aimed to explore the phytochemicals of *Digera arvensis* as carbonic anhydrase IX (CAIX) inhibitors via molecular docking and *in silico* study. The study also assesses the binding interactions, binding affinity at active site, and pharmacokinetic properties of selected phytochemicals to find the lead compounds against the hypoxia associated cancer pathways.

MATERIALS AND METHODS

Protein preparation

The crystal three-dimensional structure of CAIX (PDB ID: 8Q18) with a resolution of 2.13Åwas obtained from the Protein Data Bank (https://www.uniprot.org/). The protein was then prepared using AutoDock vina. The co-crystallized ligands and water molecules were removed. Polar hydrogen atoms were added, and Kollman charges were applied. The macromolecule was then converted to PDBQT format for docking (Khan *et al*., 2022; Hassan *et al*., 2024).

Ligand preparation

The ligands identified in the GC-MS from our previous study analysis were selected and downloaded from the PubChem (https://pubchem.ncbi.nlm.nih.gov/) in 3D SDF format. The ligands were converted to PDB format using PyMOL. Then, ligands were prepared using AutoDock Tools (1.5.7) and were then saved in PDBQT format for molecular docking.

Molecular docking and visualization

The molecular docking was performed using AutoDock Vina. The PDBQT files of protein and ligands were added into AutoDock Tools (1.5.7) for docking studies. The blind docking was performed. The top compounds with lowest binding energies were selected and was subjected to further investigation. The interactions between CAIX and the ligands were visualized and analysed by using BIOVIA Discovery Studio Visualizer, and PyMOL. To allow molecular docking of the target protein structure, a grid box consisting of 40×40×40 points with a spacing of 0.375Å was created around the active site of the target protein with the center coordinates at X = -32.685, Y = 0.534 and Z = -16.171.

Physicochemical properties

The physicochemical properties, pharmacokinetics and toxicity of the identified ligands were predicted using pkCSM and Swiss ADME web servers. The canonical SMILES of each ligand were obtained from PubChem and used for ADMET analysis. Lipinski's Rule of Five, absorption, distribution, metabolism, excretion and toxicity were evaluated to assess drug-likeness (Pires *et al*., 2015).

RESULTS

Molecular docking analysis

The binding energy for 1,3,5-Triazin-2(1H)-one, 4-amino-6-(ethylamino) was -6.1kcal/mol with a prediction of an inhibition constant of 33.78 µM. It formed hydrogen bonds with ARG46, SER182, ARG27, LEU50, ARG27, GLU49, ASN250 and displayed hydrophobic interactions with PHE189 shown in Figure 1.

1,3-Benzenedicarboxylic acid, bis(2-ethylhexyl) ester exhibited a better binding affinity of −7.9kcal/mol (Ki 1.62 µM). It made hydrogen bonds with ARG46 and numerous hydrophobic contacts with PRO47, PRO47, PHE28, LEU50 and electrostatic interactions with ARG46, ARG27, PHE189 (Table I) shown in Figure 2.

Table I. Carbonic anhydrase IX (CAIX) interaction with respective ligands from *Digera arvensis* and amino acid residues with their distances and binding properties.

Ligand name (PubChem ID)	Interactive amino acid residues (Distance: Å)			Binding energy (kcal/mol)	Inhibition constant (µM)
	Hydrogen bond	hydrophobic	Electrostatic interaction		
1,3,5-Triazin-2(1H)-one, 4-amino-6-(ethylamino) (135398734)	GLN47 (2.43) GLN47 (2.47) LYS44 (2.30)	PRO45(3.96) VAL90(4.70)		-5.8	56.05
1,3-Benzenedicarboxylic acid, bis(2-ethylhexyl) ester (8733)	LYS108 (2.89) GLN171 (1.95)	PRO45(4.39) LYS108(5.28) LYS108(4.03) LYS147(5.17) LYS147(4.78) LEU88(5.02) LEU88(4.73) LEU88(4.61) TYR178(4.99) TYR178(5.44)	LYS108(4.42) LYS108(5.12)	-6.7	12.27
1,2-Cyclohexanedicarboxylic acid, isobutyl nonyl ester (66983896)	PHE103 (2.36)	ALA63(4.16) ALA63(4.06) PRO100(5.16) VAL3(4.03)		-9.2	0.18
1,2-Cyclohexanedicarboxylic acid, 2-methylpent-3-yl nonyl ester (91722039)	PHE103(2.27) GLU46(3.53)	ALA40(4.12) ALA63(4.85) ALA63(4.36) PRO100(4.60) LYS43(4.29)		-5.2	154.30
Bis(2-ethylhexyl) phthalate (8343)	LYS108(2.51) GLN171(2.47) TYR178(2.85)	LYS108(5.48) LYS108(3.93) LYS147(5.23) LYS147(4.87) ILE111(5.08) LEU88(3.49) ILE111(5.15) TYR178(5.12) TYR178(5.42)	LYS108(4.59)	-6.7	12.27

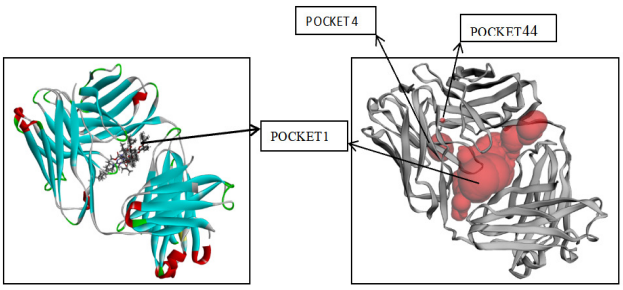


Fig. 1. Visualization of the 1,3,5-Triazin-2(1H)-one, 4-amino-6-(ethylamino) and CAIX complex. A, The representation of C1-CAIX via PyMol. B, The docked compounds showed hydrogen bonds as shown via yellow dotted lines in PyMol. C, The 2D visualization of the complex generated via DSV. D, The 3D complex generated via AutoDock vina.

Of all the compounds, 1,2-Cyclohexanedicarboxylic acid, isobutyl nonyl ester showed the highest binding affinity with a lowest binding energy of −6.8kcal/mol and an inhibition constant of 10.36 µM. It formed a hydrogen bond to GLU196, ARG86 and hydrophobic interactions to ARG252, PRO84, ILE209, ILE209 and PRO137 (Table I) shown in Figure 3.

The low binding affinity was obtained for 1,2-Cyclohexanedicarboxylic acid, 2-methylpent-3-yl nonyl ester with binding energy of – 6.7 kcal/mol (Ki 12.27 µM). It formed hydrogen bonds with GLU60,GLN175 THR125 and hydrophobic interactions with ALA23, ALA126 and LEU58 as shown in Figure 4.

Bis(2-ethylhexyl) phthalate also had a binding energy of -7.9 kcal/mol (Ki 1.62 µM). It formed multiple hydrophobic contacts with ALA23, PRO137, PHE28,

LEU and an electrostatic interaction with ARG27 (Fig. 5).

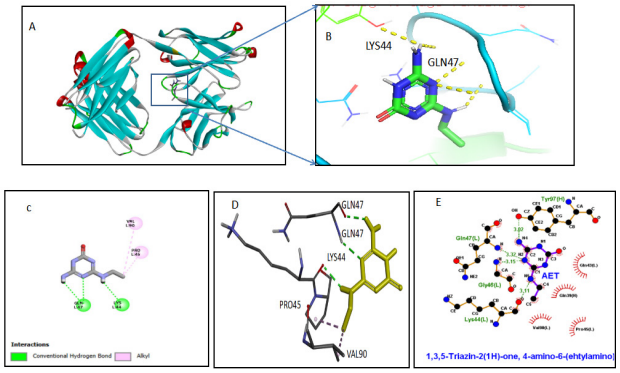


Fig. 2. Visualization of the 1,3-Benzenedicarboxylic acid, bis(2-ethylhexyl) ester and CAIX complex. A, The representation of C2-CAIX via PyMol. B, The docked compounds showed hydrogen bonds as shown via yellow dotted lines in PyMol. C, The 2D visualization of the complex generated via DSV. D, The 3D complex generated via AutoDock vina.

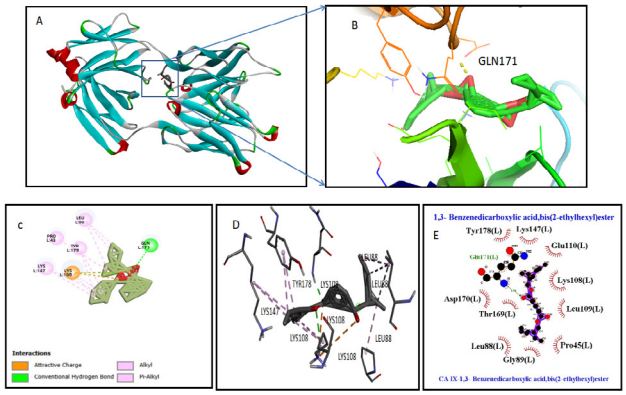


Fig. 3. Visualization of the 1,2-Cyclohexanedicarboxylic acid, isobutyl nonyl ester and CAIX complex. A, The representation of C3-CAIX via PyMol. B, The docked compounds showed hydrogen bonds as shown via yellow dotted lines in PyMol. C, The 2D visualization of the complex generated via DSV. D, The 3D complex generated via AutoDock vina.

Lipinski's rule of five

The selected phytochemicals were assessed for drug-likeness based on Lipinski's Rule of Five with respect to their molecular weight, logP, number of hydrogen bond donors and hydrogen bond acceptors (Table II) (Lipinski, 2004). The majority of compounds met with the standard drug-likeness parameters with molecular weights of less than 500 g/mol, reasonable hydrogen bond donor and acceptor properties and good physicochemical properties for oral bioavailability. Two compounds deviated somewhat (LogP>5) from the Lipinski's criteria, however. In general, most of the ligands had good drug-like properties indicative of their potential as orally active therapeutic agents (Table II).

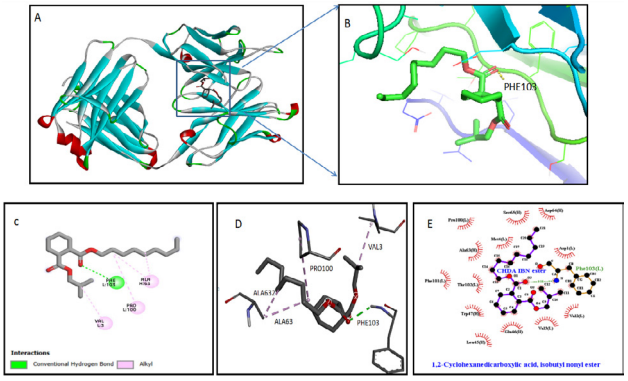


Fig. 4. Visualization of the 1,2-Cyclohexanedicarboxylic acid, 2-methylpent-3-yl nonyl ester and CAIX complex. A, The representation of C4-CAIX via PyMol. B, The docked compounds showed hydrogen bonds as shown via yellow dotted lines in PyMol. C, The 2D visualization of the complex generated via DSV. D, The 3D complex generated via AutoDock vina.

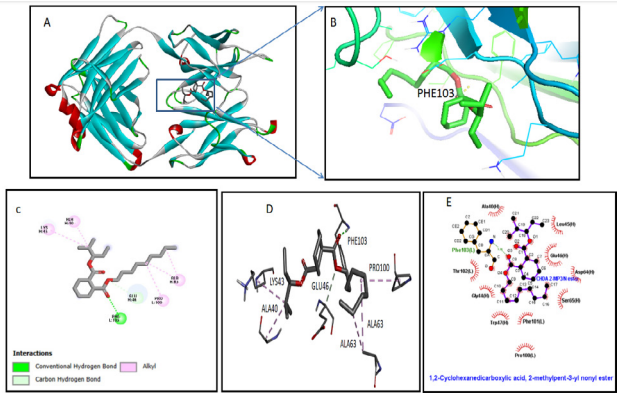


Fig. 5. Visualization of the Bis(2-ethylhexyl) phthalate and CAIX complex. A, The representation of C5-CAIX via PyMol. B, The docked compounds showed hydrogen bonds as shown via yellow dotted lines in PyMol. C, The 2D visualization of the complex generated via DSV. D, The 3D complex generated via AutoDock vina.

Drug likeness and toxicity profile

The predicted ADMET (absorption, distribution, metabolism, excretion and toxicity) properties of the selected ligands were also evaluated using the pkCSM web tool (Table III) to further establish the therapeutic potential of the selected compounds. As far as the absorption is

Table II. Lipinski rule of five analysis of selected ligands.

S. No	Ligands	Molecular weight < 500 (g/mol)	H-Bond acceptor < 10	H-Bond donors < 5	logP < 5 (WLOGP)	Polar surface area (Å²)
1	1,3,5-Triazin-2(1H)-one, 4-amino-6-(ethylamino)	155.16	5	3	0.42	96.69 Å²
2	1,3-Benzenedicarboxylic acid, bis(2-ethylhexyl) ester	390.56	4	0	5.37	52.60 Å²
3	1,2-Cyclohexanedicarboxylic acid, isobutyl nonyl ester	354.52	4	0	4.85	52.60 Å²
4	1,2-Cyclohexanedicarboxylic acid, 2-methylpent-3-yl nonyl ester	382.58	4	0	5.07	52.60 Å²
5	Bis(2-ethylhexyl) phthalate	390.56	4	0	4.77	52.60 Å²

Table III. Drug likeness prediction using pkCSM online database server for the selected ligands.

ADMET	Parameter	1,3,5-Triazin-2(1H)-one, 4-amino-6-(ethylamino)	1,3-Benzenedicarboxylic acid, bis(2-ethylhexyl) ester	1,2-Cyclohexanedicarboxylic acid, isobutyl nonyl ester	1,2-Cyclohexanedicarboxylic acid, 2-methylpent-3-yl nonyl ester	Bis(2-ethylhexyl) phthalate
Absorption	Water solubility (LogS) mol/L	-5.8	-6.491	-5.159	-5.457	-6.47
Absorption	Intestinal absorption (human) (%Absorption)	53.937	92.871	93.333	92.873	92.45
Absorption	P-Glycoprotein I inhibitors	No	No	No	No	No
Absorption	P-Glycoprotein II inhibitors	No	Yes	Yes	Yes	Yes
Distribution	VDss (human) (logL/kg)	-0.073	0.369	-0.131	-0.125	0.36
Distribution	BBB permeability	No	No	No	No	No
Distribution	CNS permeability	No	Yes	Yes	Yes	Yes
Metabolism	CYP2D6 substrate	No	No	No	No	No
Metabolism	CYP3A4 substrate	No	No	No	No	No
Metabolism	CYP2D6 inhibitor	No	No	No	No	No
Metabolism	CYP3A4 inhibitor	No	No	No	No	No
Excretion	Total clearance (Log ml/min / kg)	0.474	1.871	1.499	1.619	1.898
Excretion	Renal OCT 2 substrate	No	No	No	No	No
Toxicity	AMES toxicity categorical (Yes/No)	No	No	No	No	No
Toxicity	Max. tolerable dose (log mg/kg/day)	No	No	No	No	No
Toxicity	Hepatotoxicity	No	No	No	No	No

concerned, all the ligands showed moderate to high human intestinal absorption. The highest absorption rates observed were for 1,3-benzenedicarboxylic acid bis(2-ethylhexyl) ester (92.87%), 1,2-cyclohexanedicarboxylic acid, isobutyl nonyl ester (93.33%), 1,2-cyclohexanedicarboxylic acid, 2-methylpent-3-yl nonyl ester (92.87%) and bis(2-ethylhexyl) phthalate (92.45%), while 1,3,5-Triazin-2(1H)-one, 4-amino-6-(ethylamino) had a comparatively lower absorption of 53.94%. None of the compounds was P-glycoprotein I inhibitor but four of them (except 1,3,5-Triazin-2(1H)-one, 4-amino-6-(ethylamino)) were P-glycoprotein II inhibitors.

For distribution, none of the compounds was shown to have blood-brain barrier (BBB) permeability, decreasing the probability of adverse effects on the central nervous system (CNS). Four ligands exhibited CNS permeability according to CNS permeability parameter, however. In metabolic profiling, all 5 compounds were not found to be substrates or inhibitors of CYP2D6 and CYP3A4 enzymes indicating minimal drug–drug interaction with these

enzymes. The total clearance values of all the ligands were acceptable, the highest being bis(2-ethylhexyl) phthalate (1.898 log ml/min/kg) and the lowest was 1,3,5-Triazin-2(1H)-one, 4-amino (0.474 log ml/min/kg). All compounds showed no renal OCT2 substrate activity.

All five ligands were AMES-negative indicating no mutagenic activity and none showed hepatotoxicity, contrasting with the previous observation of Eckol in related studies. Overall, the Overall, the ADMET predictions indicate favorable absorption-related properties for the selected compounds but are insufficient to support claims of safety or oral suitability.

DISCUSSION

The present study investigated the potential interactions of selected phytochemicals identified from Digera arvensis with CAIX using molecular docking and in silico ADMET analysis. The compounds represented different chemical classes, including triazinone derivatives, benzenedicarboxylic acid esters, cyclohexanedicarboxylic acid esters, and phthalate esters. CAIX is a hypoxia-associated transmembrane zinc metalloenzyme that is overexpressed in several solid tumors, including breast, lung, renal, colorectal, and cervical cancers. It contributes to pH regulation, tumor survival, invasion, metastasis, and resistance to therapy, making it an important target for anticancer drug discovery (Supuran, 2008).

Among the five investigated compounds, 1,3-benzenedicarboxylic acid, bis(2-ethylhexyl) ester and bis(2-ethylhexyl) phthalate exhibited the strongest predicted binding affinities, with binding energies of −7.9 kcal/mol and predicted inhibition constants of 1.62μM. The 1,3-benzenedicarboxylic acid formed hydrogen bonds with ARG46, alongside hydrophobic contacts involving ARG46, PRO47, LEU50 and PHE28, as well as electrostatic interactions with ARG46, PHE189, and ARG27. Bis(2-ethylhexyl) phthalate showed multiple hydrophobic contacts with ALA23, PRO137, and PHE28, together with an electrostatic interaction involving ARG27. These predicted interactions may contribute to the binding of the compounds within the modeled CAIX structure.

1,2-Cyclohexanedicarboxylic acid exhibited a binding energy of −6.8 kcal/mol and a predicted inhibition constant of 10.36 μM. It formed hydrogen bonds with GLU196 and ARG86, together with hydrophobic interactions involving ARG252, PRO137, ILE209 and PRO84. Similarl, 2-methylpent-3-yl nonyl ester showed a binding energy of −6.7kcal/mol and a predicted inhibition constant of 12.27μM. Its predicted interactions included hydrogen bonds with GLU60, GLN175, and THR125 and hydrophobic contacts involving ALA23 and ALA126. The triazinone derivative, 1,3,5-triazin-2(1H)-one, 4-amino-6-(ethylamino), showed a binding energy of −6.1 kcal/mol and a predicted inhibition constant of 33.78μM. It formed hydrogen bonds with ASN250, ARG27, LEU50, GLU49, ARG46, SER182, and ARG27, along with a hydrophobic interaction involving PHE189. Collectively, these findings suggest differences in the predicted binding profiles of the selected compounds, although experimental enzyme inhibition assays are required to establish their actual inhibitory activity. The drug-likeness assessment based on Lipinski's rule of five indicated that most compounds met the evaluated physicochemical criteria, although two compounds exceeded the recommended logP threshold. The ADMET predictions suggested moderate to high intestinal absorption across the selected compounds. None was predicted to cross the blood–brain barrier, although some showed predicted central nervous system permeability according to the separate CNS permeability parameter. The compounds were also predicted to be AMES-negative and non-hepatotoxic, with no predicted renal OCT2 substrate activity. These computational predictions provide preliminary information about their pharmacokinetic and toxicity profiles but do not establish that the compounds are safe or suitable for oral administration in humans.

Overall, the docking and ADMET results identify several D. arvensis-associated compounds worthy of further investigation as potential CAIX-targeting candidates. The two compounds with binding energies of −7.9 kcal/mol may warrant particular attention in subsequent studies. Nevertheless, experimental validation is essential to determine whether the predicted interactions translate into measurable CAIX inhibition and biologically relevant anticancer effects.

Limitations

While the results of the present study are encouraging, there are some limitations. *In vitro* and *in vivo* results can be different from the binding affinities and pharmacokinetic properties predicted by computational methods, which can only simulate biological systems, the complexity of which cannot be fully captured by such methods (Morris *et al*., 2009). Docking is highly algorithm and score function dependent and may not always agree with experimental data. Further, it is important to note that the present study examined only the five selected phytochemicals of *Digera arvensis* as reported in literature, but more thorough phytochemical analysis, using techniques like LC-MS could yield further bioactive compounds with better therapeutic potential. In addition, no molecular dynamics simulations were carried out to assess long-term stability and conformational flexibility of the ligand-CAIX

complexes. Thus, more experimental evidence is needed before definitive clinical conclusions can be drawn.

Future recommendations

Further studies are needed to investigate the complete phytochemical characterization of *Digera arvensis* by advanced analytical methods like LC-MS to discover more bioactive compounds with inhibitory activity against CAIX. *In silico* screening and molecular dynamics simulation should be extended and used to assay stability, conformation and binding potency of the highest potential compounds in the future. Especially 1,3-benzenedicarboxylic acid, bis(2-ethylhexyl) ester and bis(2-ethylhexyl) phthalate should be targeted for further investigation due to its higher docking score. Furthermore, the biological activity of these compounds, their pharmacokinetic properties and their safety profile must be assessed in a variety of in vivo assays in appropriate animal models and in enzyme inhibition assays to confirm the activity of these compounds. Experimental toxicity assessment (including endocrine, reproductive and hepatic endpoints) should precede any *in vivo* efficacy work, and DEHP should be prioritized only as a reference binder, not as a lead compound. A combination of computational and experimental strategies will aid in the development of *Digera arvensis*-based phytochemicals for the treatment of hypoxia-related cancers.

CONCLUSION

Finally, the present study conducted extensive molecular docking and *in silico* docking study on phytochemicals of *Digera arvensis* with Carbonic Anhydrase IX (CAIX) (PDB ID: 8Q18). All the compounds investigated showed favorable predicted binding energies toward CAIX in docking; inhibitory activity remains to be confirmed experimentally. 1,3-benzenedicarboxylic acid, bis(2-ethylhexyl) ester and bis(2-ethylhexyl) phthalate was found to have the highest binding affinity and strongest interaction profile with the CAIX active site of the tested ligands and is therefore a promising lead compound for the development of anticancer drugs. The in silico pharmacokinetic predictions were favorable for most compounds, but toxicity predictions conflict with known experimental toxicology for DEHP and cannot establish safety. These results provide a computational basis for experimental CAIX inhibition assays and toxicological evaluation, not evidence of therapeutic suitability. In general, the results of this study give a useful computational basis for experimental testing and suggest the possibility of the use of *Digera arvensis* phytochemicals as anticancer drugs in the treatment of CAIX related hypoxic tumors.

DECLARATIONS

Acknowledgement

The authors would like to express their sincere gratitude to the Cancer Research Lab, Institute of Zoology, University of the Punjab, Quaid-e-Azam Campus, Lahore, Pakistan, for providing the necessary facilities, computational resources, and research environment to conduct this study.

Funding

The study receives no funding.

Generative AI and AI assisted technology statement

The authors declare that no generative AI and AI assisted technology was used in the creation of this manuscript.

Statement of conflict of interest

The authors have declared no conflict of interest.

REFERENCES

Ali, M., Hilvo, M., Di Fiore, A., Supuran, C.T., Pan, P., Parkkila, S., Scaloni, A., Pastorek, J., Pastorekova, S., Pedone, C., Scozzafava, A., Monti, S.M. and De Simone, G., 2024. Phytochemical and pharmacological activities of Digera arvensis: A comprehensive review. *J. Ethnopharmacol*., **315**: 116–128. https://doi.org/10.1073/pnas.0908301106

Alterio, V., Hilvo, M., Di Fiore, A., Supuran, C.T., Pan, P., Parkkila, S., Scaloni, A., Pastorek, J., Pastorekova, S., Pedone, C., Scozzafava, A., Monti, S.M. and De Simone, G., 2009. Crystal structure of the catalytic domain of the tumor-associated human carbonic anhydrase IX. *Proc. natl. Acad. Sci*., **106**: 16233–16238. https://doi.org/10.1073/pnas.0908301106

Alterio, V., Langella, E., De Simone, G. and Monti, S.M., 2022. Carbonic anhydrase IX structure and function in hypoxic tumors. *Curr. Pharma. Design*, **28**: 1022–1035.

Cheung, S.M. and Chenoweth, D.M., 2023. Carbonic anhydrase IX as a therapeutic target in solid tumors: Current status and emerging strategies. *Cancer Treatment Rev*., **115**: 102523.

Ferreira, L.G., Dos Santos, R.N., Oliva, G. and Andricopulo, A.D., 2022. Molecular docking and structure-based drug design strategies in drug discovery. *Molecules*, **27**: 4723.

Jing, X., Yang, F., Shao, C., Wei, K., Xie, M., Shen, H. and Shu, Y., 2023. Role of hypoxia in cancer

therapy by regulating the tumor microenvironment. *Mol. Cancer*, **22**: 1–15.

Hassan I., Zaman A., Zafar E. and Khan M., 2024. Molecular docking-aided identification of natural bioactive molecules as potential cancer cell proliferation inhibitors: Molecular docking as cancer cell inhibitors. *Futuri. Biotechnol.,* **30**:25-30.

Khan, A., Khan, SU., Khan, A., Shal, B., Rehman, SU., Rehman, SU., Htar, TT., Khan, S., Anwar, S., Alafnan, A. and Rengasamy, KR., 2022. Anti-inflammatory and anti-rheumatic potential of selective plant compounds by targeting TLR-4/AP-1 signaling: A comprehensive molecular docking and simulation approaches. *Molecules,* **27**(13): 4319.

Khan, Y., Naz, A., Ullah, A., Mujib, G., Khan, L., Shoukat, M., Abdelmohsen, SA., Alenzai, MA., Naseem, MT. and Kamal, A., 2024. Identification of PI3K alpha inhibitors through large-scale virtual screening and integrated molecular modeling, biophysical characterization, and ADMET profiling. *Scienti. Rep.,* **16**(1):20802.

Kumar, A., Singh, A. and Chandra, R., 2023. Natural products as anticancer agents: A review of phytochemical-based drug discovery. *Phytochem. Rev*., **22**: 789–820.

Lionta, E., Spyrou, G., Vassilatis, D.K. and Cournia, Z., 2023. Structure-based virtual screening for drug discovery: Principles, applications and recent advances. *Curr. Topics Med. Chem*., **14**: 1923–1938. https://doi.org/10.2174/1568026614666140929124445

Lipinski, C.A., 2004. Lead- and drug-like compounds: The rule-of-five revolution. *Drug Discov. Today: Technol*., **1**: 337–341. https://doi.org/10.1016/j.ddtec.2004.11.007

Mboge, M.Y., Mahon, B.P., McKenna, R. and Frost, S.C., 2022. Carbonic anhydrases: Role in pH control and cancer. *Metabolites*, **8**: 19. https://doi.org/10.3390/metabo8010019

McDonald, P.C., Chia, S., Bedard, P.L., Chu, Q., Lyle, M., Tang, L., Singh, M., Zhang, Z., Supuran, C.T., Renouf, D.J. and Dedhar, S., 2023. A phase 1 study of SLC-0111, a novel inhibitor of carbonic anhydrase IX, in patients with advanced solid tumors. *Am. J. clin. Oncol*., **43**: 484–490. https://doi.org/10.1097/COC.0000000000000691

Morris, G.M., Huey, R., Lindstrom, W., Sanner, M.F., Belew, R.K., Goodsell, D.S. and Olson, A.J., 2009. AutoDock4 and AutoDockTools4: Automated docking with selective receptor flexibility. *J. Comput. Chem*., **30**: 2785–2791. https://doi.org/10.1002/jcc.21256

Pastorekova, S., Gillies, R.J. and Bhujwalla, Z.M., 2023. The role of carbonic anhydrase IX in tumor biology and therapy. *Curr. Pharma. Design*, **29**: 745–758.

Patel, H.M., Pawara, R., Ansari, A. and Noolvi, M., 2023. Recent updates on structure-based and ligand-based virtual screening for rational drug design. *Curr. Topics Med. Chem*., **18**: 1628–1654.

Pires, D.E.V., Blundell, T.L. and Ascher, D.B., 2015. pkCSM: Predicting small-molecule pharmacokinetic and toxicity properties using graph-based signatures. *J. med. Chem*., **58**: 4066–4072. https://doi.org/10.1021/acs.jmedchem.5b00104

Rahman, M.M., Khan, S., Khan, O., Hayat, U., Nisar, S., Waqar, M., 2023. Ethnobotanical and pharmacological properties of Digera arvensis Forssk.: A review. *Asian Pac. J. Trop. Biomed*., **13**: 193–204.

Rankin, E.B. and Giaccia, A.J., 2022. Hypoxic control of metastasis. *Science*, **352**: 175–180. https://doi.org/10.1126/science.aaf4405

Semenza, G.L., 2022. The hypoxic tumor microenvironment: A driving force for breast cancer progression. *Biochim. Biophys. Acta Mol. Cell Res*., **1863**: 382–391. https://doi.org/10.1016/j.bbamcr.2015.05.036

Supuran, C.T., 2008. Carbonic anhydrases: Novel therapeutic applications for inhibitors and activators. *Nat. Rev. Drug Discov*., **7**: 168–181. https://doi.org/10.1038/nrd2467

Supuran, C.T., 2023. Carbonic anhydrase inhibitors as emerging agents for the treatment and imaging of hypoxic tumors. *Exp. Opin. Invest. Drugs*, **32**: 1–15.

Vaupel, P. and Multhoff, G., 2022. Fatal alliance of hypoxia-/HIF-1α-driven microenvironmental traits promoting cancer progression. *Adv. exp. Med. Biol*., **1232**: 169–176. https://doi.org/10.1007/978-3-030-34461-0_21

Zhang, Y., Chen, X., Gueydan, C. and Han, J., 2024. Plasma membrane changes during programmed cell deaths. *Cell Res*., **28**: 9–21. https://doi.org/10.1038/cr.2017.133